Gas-Phase Unfolding and Disassembly Reveals Stability Differences in Ligand-Bound Multiprotein Complexes

Suk-Joon Hyung,[1] Carol V. Robinson,[1,*] and Brandon T. Ruotolo[1,*]
[1]Department of Chemistry, University of Cambridge, Lensfield Road, Cambridge CB2 1EW, UK
*Correspondence: cvr24@cam.ac.uk (C.V.R.), btr23@cam.ac.uk (B.T.R.)
DOI 10.1016/j.chembiol.2009.02.008

SUMMARY

Mass spectrometry (MS) is widely used to assess the binding of small molecules to proteins and their complexes. In many cases, subtle differences in the stability afforded by binding of ligands to protein assemblies cannot be detected by MS. Here we show that monitoring the unfolding of protein subunits, using ion mobility-MS, allows differentiation of the effects of ligand binding not normally observed by MS alone. Using wild-type and disease-associated variants of tetrameric transthyretin, MS data indicate that populations of the variant protein are less stable than wild-type. Ion mobility-MS, however, is able to show that the natural ligand of transthyretin, thyroxine, provides a larger stability increase to the tetramer composed of variant subunits than to the wild-type protein-ligand complex. Overall, therefore, our results have implications for small-molecule drug design directed at multiprotein targets.

INTRODUCTION

The analysis of protein-ligand complexes by mass spectrometry (MS) has a long history, from the earliest demonstrations of protein-ligand complexes in which the intensity of ions was used, in some cases, to correlate binding affinity (Ganem et al., 1991; Katta and Chait, 1991; Hu and Loo, 1995) through to more recent applications to multiprotein complexes (McCammon et al., 2002; Kitova et al., 2008). These latter studies were able to demonstrate the effect of ligand binding on the overall stability of the protein complex in the gas phase. The addition of tandem MS to the study of protein-ligand complexes provides further insight into their stability (Shoemaker et al., 2007). Tandem MS typically involves activation of a narrow m/z (mass/charge) region representing the protein complex of interest, selected using a primary mass filter (e.g., a quadrupole). Subsequent monitoring of fragment ions can be carried out with a time-of-flight or other mass analyzer. A common method for activating ions is collision-induced dissociation (CID), whereby the selected ions are subjected to collisions with neutral gas molecules. Protein complex ions activated in this way generally undergo unimolecular dissociation, and the mechanism of their dissociation has been the subject of much research (Felitsyn et al., 2001, 2002; Jurchen and Williams, 2003; Jurchen et al., 2004).

There are several mechanistic aspects of gas-phase protein complex dissociation that have been established. For example, the predominant fragmentation pathway for most protein complexes involves expulsion of monomeric protein in a sequential fashion to give both highly charged subunits and lowly charged, multiply "stripped" complex ions (Light-Wahl et al., 1994). Also, experimental and theoretical data indicate that a degree of protein unfolding precedes dissociation (Felitsyn et al., 2001, 2002; Jurchen and Williams, 2003; Jurchen et al., 2004; Ruotolo et al., 2007). A positive correlation has been proposed between the charges accumulated on the fragment ions and estimates of their exposed surface area. This indicates that whereas the charge partitioning that occurs during the dissociation process is "asymmetric" with respect to mass, it is symmetric with respect to the surface area of the ion (Benesch et al., 2006).

In the case of an intact assembly composed of a protein complex and a small-molecule ligand, minimal activation of the assembly is often sufficient to dissociate the ligand. This dissociation is generally favored in protein complexes where the subunits and ligands are maintained by hydrophobic interactions (Robinson et al., 1996; Loo, 1997), although data indicate that even this basic rule has exceptions (Bovet et al., 2007). Although the analysis of the gas-phase structure of protein-ligand complexes was not the focus of these early reports, recent developments that involve coupling ion-mobility separation in tandem with mass spectrometry (IM-MS) enable the gas-phase structure of protein complexes to be assessed. IM is a technique that separates gas-phase species by their ability to traverse a chamber filled with neutral gas molecules under the influence of a weak electric field (von Helden et al., 1995; Hoaglund-Hyzer et al., 1999; Jarrold, 2000; Ruotolo et al., 2005). Extended ions will undergo collisions with neutral gas molecules more frequently than compact ions, and will thus be separated according to their overall differences in shape and size by IM-MS. Using such an approach, it was demonstrated that many features of protein complex structure are retained in the absence of bulk solvent (Ruotolo et al., 2005; Ruotolo and Robinson, 2006).

In a previous study, the influence of collisional activation on the folded state of tetrameric transthyretin (TTR), a protein implicated in familial amyloid polyneuropathy, showed that increasing the internal energy of the protein complex resulted in ions that
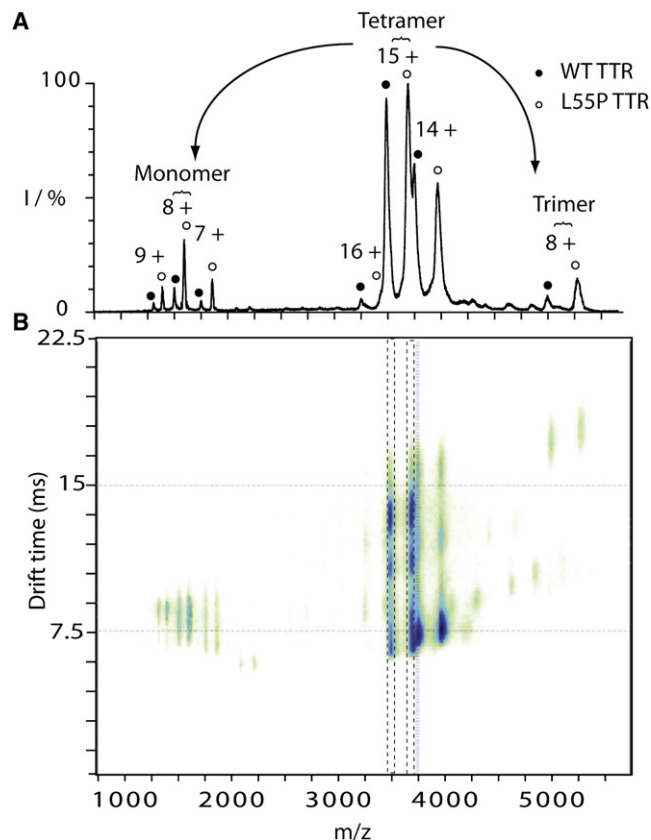
Figure 1. Ion Mobility-Mass Spectrometry Data for WT and L55P TTR
(A) Mass spectra of wild-type [^{12}C-^{14}N] TTR and L55P [^{13}C-^{15}N] TTR acquired at a trap collision voltage of 40 V. Peaks corresponding to 14–16+ charge states of tetramer, 7–9+ charge states of monomer, and 8+ trimer ions of transthyretin are shown.
(B) A contour plot of m/z versus drift time is shown. A narrow window that contains only 15+ ions of wild-type (3720 m/z) or L55P (3800 m/z) TTR tetramer is highlighted on a contour plot of m/z versus drift time (dotted box). Again, the monomer ion signal is also observed at low m/z. No significant CCS differences are observed between WT and L55p monomers.

have undergone moderate to extensive unfolding, while maintaining their tetrameric state (Ruotolo et al., 2007). In addition, MS studies on TTR have indicated that several point mutations decrease the overall stability of the gas-phase quaternary structure of TTR, in agreement with solution-phase data (Nettleton et al., 1998). Moreover, a previous investigation of small-molecule ligands binding to the TTR tetramer produced a rank order of 18 ligands and identified cooperativity of binding not reported previously (McCammon et al., 2002). Such small ligands bind to the hydrophobic interface of TTR and stabilize the tetrameric assembly by raising the energetic barrier for dissociation into monomers (Hammarstrom et al., 2003). Although it is possible to assess by mass spectrometry when ligands are lost from protein assemblies, the overall effects on the stability and dissociation pathways of the apo versus holo complexes are not always apparent.

In this report, we investigate the gas-phase unfolding and dissociation of ligand-bound TTR and its variant forms by IM-MS. We employ variants of TTR labeled with stable isotopes

so that wild-type (WT) TTR can be introduced as a reference under the same instrument conditions as the variant. We examine the well-characterized natural hormone thyroxine, for which TTR functions as a carrier protein in vivo and which has been shown previously to be effective at inhibiting amyloid fibril formation (Klabunde et al., 2000). Our experiments allow us to address the influence of partially ligated states of WT or variant TTR because the mass differences afforded by isotope labeling and/or ligand binding enables us to select a single population of protein complex prior to IM-MS. In this way, we can examine and differentiate the influence of ligands or mutations on the stability of TTR without concern for the differential formation, transmission, and activation of ions.

Our results show that a point mutation in the protein sequence is effective at decreasing the stability of subunit contacts without significantly influencing the extent of unfolding. In contrast, the natural ligand of TTR, thyroxine, acts to suppress unfolding of each of the subunits significantly, and increases the energy required to unfold the complex. Together, these data show that a protein complex can be characterized not only by the extent of either unfolding or dissociation but also by analyzing the relationship between these two information sets. This is an exciting result, demonstrating that MS and IM present orthogonal information on the stability of the quaternary and tertiary/secondary structures of the protein complex, respectively. Furthermore, in this study, we provide a comprehensive view of the dissociation of TTR that is particularly relevant for assessing the effects of point mutations and ligand binding.

RESULTS AND DISCUSSION

Measuring both Protein Unfolding and Dissociation Using IM-MS
To understand the factors that influence the stability of both quaternary and tertiary structures of transthyretin in the gas phase, L55P TTR, a variant form of TTR of lower stability than the WT TTR (Lashuel et al., 1998; Nettleton et al., 1998), was studied. L55P TTR is a pathogenically aggressive point mutant known to undergo subunit exchange 10-fold faster than WT TTR (Lashuel et al., 1998; Keetch et al., 2005). Interestingly, this occurs despite similar arrangements of subunits and their interfaces revealed by X-ray crystallography (Sebastiao et al., 1996). In order to resolve by MS the WT and L55P variant TTR, and consequently to ensure that both protein complexes experience the same experimental conditions, we used an L55P TTR sample uniformly labeled with stable carbon and nitrogen isotopes and compared it with the wild-type protein containing isotopes of natural abundance.

A mass spectrum of an equimolar solution of WT [^{12}C-^{14}N]TTR and L55P [^{13}C-^{15}N]TTR is shown in Figure 1A. A pair of peaks at 3720 and 3900 m/z correspond to the 15+ charge states of WT and L55P TTR tetramers, respectively. The mass spectrum also shows minor peaks corresponding to 14+ and 16+ charge states of tetrameric TTR. Under the conditions used to acquire the data (trap collision voltage = 40V), we observe a small fraction of tetramer dissociating into monomer and trimer (Figure 1), indicative of collision-induced dissociation of the TTR tetramer as reported previously (Nettleton et al., 1998). Monomeric L55P TTR is more abundant than monomeric WT
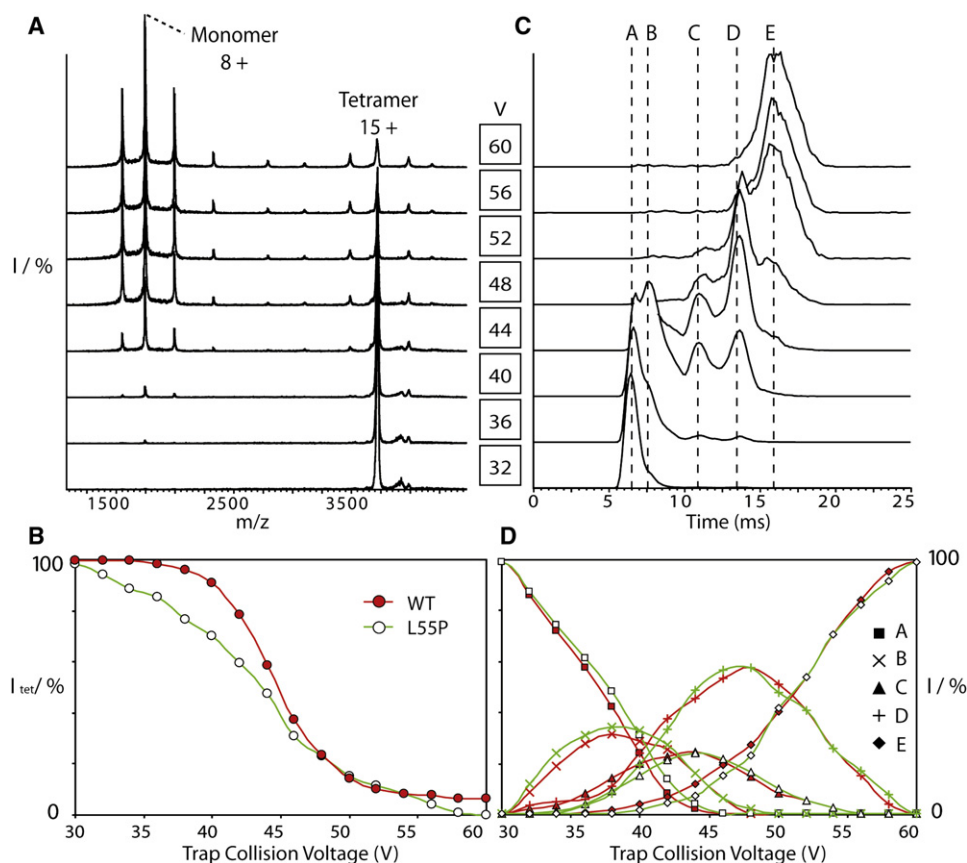
Figure 2. Dissociation and Unfolding of WT TTR

(A) The complete mass spectrum of the 15+ charge state of wild-type [^{12}C-^{14}N]TTR tetramer ions selected by the quadrupole mass filter (3720 ± 12 m/z). Trap collision voltage (V) was applied to the ions in the trapping region between the quadrupole mass analyzer and ion-mobility cell. Major peaks from charge state series corresponding to monomeric and tetrameric TTR are labeled.

(B) The relative intensities of wild-type (filled) and L55P (open) tetrameric TTR, I_{tet}, are shown against trap collision voltage.

(C) The arrival time distributions of the 15+ charge state of WT TTR tetramer acquired at the corresponding trap collision voltage show a transition from compact to extended ion conformations. The centroid collision cross-sections of peaks are labeled from A to E (A: 2950; B: 3250; C: 3800; D: 4300; E: 4700 Å^2).

(D) The relative intensities of the individual peaks calculated from the arrival time distribution of 15+ charge state of tetramer of wild-type (filled) and L55P TTR (open).

TTR when exposed to the same experimental conditions, consistent with the observation that its reduced subunit integrity correlates with amyloidogenicity (Nettleton et al., 1998).

Drift times for the ions were acquired under the same conditions as above and are shown in a plot of drift time versus m/z (Figure 1B). The plot shows a number of peaks resolved in the drift time dimension corresponding to the tetrameric charge state series of WT [^{12}C-^{14}N]TTR and L55P [^{13}C-^{15}N]TTR. At 3720 and 3900 m/z, which correspond to 15+ charge states of WT and L55P TTR tetramer populations, respectively, we observe a number of peaks extended over the drift time dimension. This indicates that the tetramers exist in a range of structural states at this activation energy (600 eV laboratory-frame energy). We assign these to partially unfolded states of tetramers which are stable over the timescale of drift tube separation (30 ms), consistent with long-lived intermediates produced from the activated 15+ charge state of TTR tetramer (Ruotolo et al., 2007). At this point, even though tetramers are present in a broad range of structural states the ions are largely intact, indicated by

the observation that <10% of the total ion current is carried by fragment ions. Therefore, taking the mass spectrum and contour plot together, we can monitor not only the conversion from tetrameric into monomeric and trimeric dissociation products but also their conversion from folded into unfolded tetramer ions.

An Amyloidogenic Variant Dissociates More Readily

In order to investigate the stability of WT and L55P TTR over a wide range of activating conditions, we obtained IM-MS data for a solution containing both WT and L55P TTR across a range of trap collision voltages and examined their conversion from tetrameric/folded states to dissociated/unfolded states, respectively. The dissociation of TTR tetramer is demonstrated from mass spectra of the 15+ charge state of WT tetrameric TTR acquired over a range of trap collision voltages (Figure 2A). Similar mass spectra were recorded for L55P TTR (data not shown). Using a low trap collision voltage, the original tetramer population is intact along with a small amount of ion current corresponding to the 14+ tetramer. This ion population is the result

of charge stripping, a facile decay pathway for large protein complexes that has been reported previously (Jurchen and Williams, 2003). Increasing the trap collision voltage results in the formation of monomer and trimer (trimer not shown). We also observe the appearance of a minor signal corresponding to 16+ charge state of tetramer due to loss of negatively charged counterions from 15+ charge state of tetramers (Sobott and Robinson, 2004). The intensity of tetramer and monomer allows us to estimate the conversion from tetrameric to monomeric states of TTR.

To compare the gas-phase stabilities of the WT and variant TTR populations, we monitored the dissociation of the tetramer as a function of trap collision voltage by MS. From these MS data, the intensity of the peaks corresponding to TTR relative to those of monomeric transthyretin was calculated and is defined as I_{tet}. We then constructed a plot of I_{tet} versus the trap collision voltage for the 15+ charge state of tetrameric WT and L55P TTR (Figure 2B). From this plot, we deduce that L55P TTR dissociates to a greater degree relative to WT TTR, with a maximum difference in the intensity of WT and L55P TTR tetramers observed at trap collision voltages below 45 V. The difference between WT and L55P tetramers decreases with elevated trap collision voltage and becomes insignificant beyond 50 V. The results presented clearly show that the conversion from tetramer to monomer of L55P TTR is consistently greater than the analogous dissociation pathway of WT TTR.

A Common Unfolding Pathway for Transthyretin and Its Disease-Associated Variants

The arrival time distribution acquired for the 15+ charge state of tetrameric WT TTR using low trap collision voltage shows a narrow peak that corresponds well to the collision cross-section (CCS) calculated for a compact TTR tetramer ($\sim$2950 Å^2). As the trap collision voltage is increased, a number of broad but discrete peaks increase in intensity at longer drift times (Figure 2C). We assign these peaks to unfolded states of the TTR tetramer as reported previously (Ruotolo et al., 2007). For the purpose of this study, we have arbitrarily labeled these as different conformational ensembles A–E in order of their increasing CCS values. The intensity of the peak that corresponds to the compact tetramer (A) (2950 Å^2) begins to decrease beyond a trap collision voltage of 36 V, B becomes prevalent (3250 Å^2), followed by C (3800 Å^2) and D (4300 Å^2) at 44–52 V. At 60 V, the most extended tetramer, E (4700 Å^2), is the major conformational ensemble observed. No further changes in the arrival time distribution are observed beyond 60 V, and only a small population of the intact tetramer can be observed in the mass spectrum (Figure 2A). The width of peak E is considerably broader relative to the other peaks, suggesting that a larger number of disparate conformations populate peak E compared with peaks A–D. We observed similar arrival time distributions with conformational ensembles of similar size from L55P TTR (see Supplemental Data available online).

To compare the gas-phase unfolding of the WT and L55P tetramers, the relative intensities of the five different conformational ensembles were plotted for each trap collision voltage value (Figure 2D). For both proteins, the conformational ensemble B is produced to a maximum level at 36 V whereas the intensities of partially unfolded ensembles C and D rise in

abundance concurrently until 42 V, after which D is more abundant. The most unfolded tetramer ensemble, E, is not accessed until the compact states in A account for less than 5% of the total ion current. Taking the arrival time and the intensity plot together, we show that activated WT or L55P TTR tetramers generate unfolded populations of nearly identical CCS upon activation in the gas phase. In order to see whether these conformational ensembles are conserved across other variants of TTR, we studied TTR with point mutations that either stabilize (T119M) or destabilize (V30M) the TTR tetramer. Using the same approach described above for L55P TTR, we compared the stability of the variant with respect to the wild-type protein. Interestingly, IM-MS data for these variants are similar to both the WT and L55P data shown in Figure 2D (Supplemental Data). Overall, these data show that point mutations have little effect on the unfolded ensembles observed in the gas phase for TTR.

Comparing the effects of activation on both the gas-phase dissociation and unfolding of tetrameric TTR highlights the orthogonal nature of MS and IM data sets. IM data chart the nearly identical unfolding for the two complexes. In contrast, MS data indicate a significant difference between the stability of WT and L55P TTR. Therefore, these data together imply that WT and L55P tetramer form dissociation products via different routes. For example, the folded WT tetramer population must decrease to $\sim$50% intensity for significant dissociation to occur. In contrast, dissociation of a subunit from the L55P tetramer occurs while the folded population constitutes a significantly larger proportion of tetrameric TTR ($\sim$80%). This line of analysis implies that the monomers ejected from L55P tetramers are, initially, more folded on average than those from WT tetramers, and further implies that the intersubunit interactions in the L55P tetramer are weaker than those within WT TTR.

Small-Molecule Ligand Binding to TTR Delays Unfolding

To study the influence of small-molecule ligand binding on the unfolding and dissociation of the tetrameric assembly in the gas phase, we analyzed a solution of WT TTR with its natural ligand thyroxine at a concentration of 3.24 μM ligand in 3.6 μM TTR tetramer solution. TTR tetramers exist in three different binding states in solution under these conditions: unbound (apo-TTR), singly ligated (TTR-L), and doubly ligated (TTR-L$_2$), at the ratio 35%:40%:25% determined from the dissociation constant measured in solution (Nilsson et al., 1975; Blake et al., 1978). A mass spectrum for the WT TTR-ligand complex acquired under conditions that maintain interaction with ligands (low trap collision voltage) is shown (Figure 3A). A set of triplet peaks are observed for each of the charge states 11+ to 16+ attributed to tetrameric apo-TTR, TTR-L, and TTR-L$_2$ (inset shows an expansion of the 15+ charge state). The relative intensity of peaks representing the three TTR complexes is in close agreement with predictions from dissociation constants in solution. IM data show only a single narrow distribution of tetramer ions for all charge states at low trap collision voltage (Figure 3B). These narrow arrival time distributions indicate that TTR-L and TTR-L$_2$ are retained as compact protein-ligand assemblies in the gas phase.

The stability of an individual apo or ligand-bound state of the tetramer was assessed by selecting a narrow m/z range in the quadrupole mass filter, corresponding to either apo-TTR or
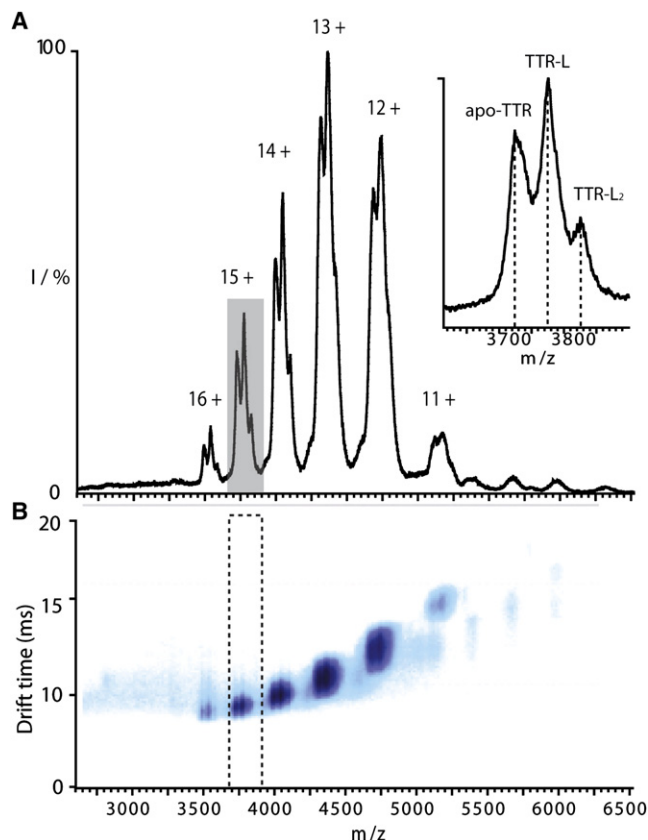
Figure 3. Mass Spectra of WT TTR with Thyroxine

(A) Mass spectra of WT TTR with thyroxine under nonactivating instrument conditions (trap collision voltage = 30 V) shows a distribution of a triplet of peaks corresponding to 11–16+ charge states of apo-tetramer, and holo-tetramer with one and two ligands. Inset: a close-up of 15+ charge states of apo- and holo-TTR tetramers with dotted lines on the centroids of peaks chosen for mass selection experiments (3720, 3775, and 3825 m/z, respectively).

(B) Ion mobility-mass spectrometry data of the tetramer shows a narrow distribution of drift time for all apo and TTR-ligand complexes.

TTR-L or TTR-L_2. The resulting ion population was then subjected to IM-MS analysis, and the arrival time distributions recorded for the 15+ charge state of each ligand-bound state of the tetramer are shown (Figure 4A). A compact protein-ligand assembly is seen for all binding states. When activated, the arrival time distributions of apo-TTR, TTR-L, and TTR-L_2 complexes all show additional peaks at longer drift times (Figure 4B). We note that, at fixed trap collision voltages, the relative abundance of the most compact conformational ensemble A from TTR-L or TTR-L_2 is significantly increased compared to that of apo-TTR. There is, however, a clear reduction in the relative intensity of the partially unfolded tetramers C and D when ligand is bound.

An in-depth analysis, involving the generation of contour plots of trap collision voltage against the observed drift time of apo-TTR and TTR-L_2, reveals several subtle differences between the two protein complexes (Figures 4C and 4D). These plots can be viewed as an IM-MS "fingerprint" for a specific protein complex. Upon comparison, both the drift time and the order of the five major peaks observed are conserved between the

apo and holo forms of the complex. This indicates that a similar unfolding pathway exists that is independent of ligand binding. The primary difference between the two contour plots is, however, that each conformational ensemble appears at higher voltage values for TTR-L_2 relative to apo-TTR. This shift, as discussed in the next section, is of primary importance, and conveys information on the stability conferred to the tetramer upon ligand binding that is not present in MS data alone. There are also some intriguing minor differences that can be observed upon comparing Figures 4C and 4D. The boxed region shows that the breadth of the features are elongated in the TTR-L_2 plot (Figure 4D) when compared to the TTR plot (Figure 4C). This difference is assigned to structural transitions that occur upon activation of TTR-L_2 that occur to a lesser extent in apo-TTR. Comparison of the data from holo and apo states of TTR may also confer a detailed picture of how ligands provide stability to the protein assembly that has yet to be fully understood. For example, the data in Figures 4C and 4D indicate that ligand binding can stabilize not only the most compact conformational ensemble but also other partially folded structures. This observation may imply that ligand binding does not require an optimal binding pocket in order to form hydrophobic contacts. Significantly, the data demonstrate the sensitivity of this IM-MS fingerprinting to subtle changes in unfolding of a multiprotein complex.

Decoupling Unfolding from Dissociation

In order to determine quantitatively the stability afforded to the TTR tetramer as a result of ligand binding, a simplified descriptor of tetramer unfolding was calculated as a fraction of the folded tetramer A over the sum of all conformational ensembles A–E, termed I_f to denote the intensity of the folded state. In addition, the proportion of intact tetramers versus monomers was estimated from the tandem MS spectra for the same range of trap collision voltages, and termed I_{tet} as defined previously.

A plot of I_f and I_{tet} for 15+ charge state of WT TTR in three different ligand-binding states as a function of trap collision voltage is shown (Figure 5A). Both I_f and I_{tet} follow typical decay curves as a function of the activating voltage. We note that, as anticipated, I_f decreases prior to I_{tet} in all binding states of the wild-type protein. Ligand binding, however, causes a small shift of I_f toward higher voltages without changing the rate of decay. I_f is also energetically well separated from I_{tet}, implying that dissociation occurs after significant unfolding on the tetramer in the gas phase. In contrast, the analogous data set for L55P TTR shows that I_{tet} initially decreases more rapidly at low activation voltages, at which point I_{tet} and I_f are of comparable intensity (Figure 5B). As a result of this earlier onset of dissociation, I_{tet} is reduced at lower activating voltage for L55P when compared to WT TTR. Interestingly, ligand binding does not influence the onset of decay for I_{tet}. This is likely due to weaker protein-ligand interactions in the TTR-ligand complex compared with the protein-protein interactions between subunits. Importantly, however, ligand binding to the L55P tetramer shifts the decay curve of I_f significantly, implying that a greater degree of folding is maintained by ligand binding to L55P than to WT TTR.

This result is further illustrated by a comparison of the dissociation energy at which the intensity of folded tetramer or the population of tetrameric TTR reduces to 50% (Figure 5C). Whereas
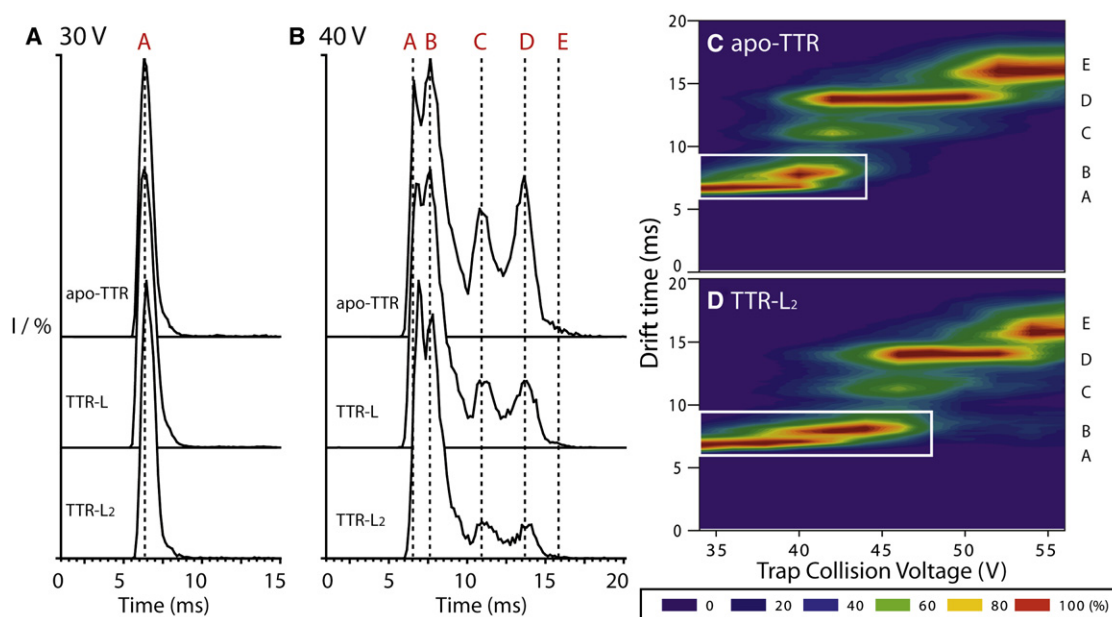
Figure 4. Ion-Mobility Data of WT TTR with Thyroxine

Arrival time distributions of 15+ apo-TTR tetramer (TTR), holo-tetramer with one (TTR-L) and two ligands (TTR-L$_2$) ions at trap collision voltages of 30 V (A) and 40 V (B) are shown. Tetramer-ligand complexes from Figure 3 were selected at quadrupole mass filter and activated prior to separation in the ion mobility cell. The centroids of peaks are labeled. A voltage ramp experiment at the transfer region prior to IM-MS is represented as a contour plot of arrival time distribution against trap collision voltage ([C] and [D], TTR and TTR-L$_2$, respectively). Compact and partially unfolded tetramer A and B are highlighted (white box) showing an extended population of ligand-bound tetramers across a larger range of collision voltages.

the apo form of either WT or L55P TTR tetramer requires similar energy to unfold, IM data recorded for WT TTR indicate that the onset of unfolding gradually increases upon successive ligand-binding events. The energy required for dissociation for WT TTR measured by MS remains unaffected within an experimental error of ±5 eV (Figure 5C). Similar trends are observed for L55P TTR. However, in this case, the occupancy of binding sites in L55P TTR protects the protein from unfolding at higher activation energies than in the case of WT TTR. This observation is further confirmed by a steeper slope for the positive correlation between 50% unfolding yield and the number of ligands bound to L55P TTR (23.8 eV per addition of a ligand) when compared with WT TTR (11.2 eV per addition of a ligand). These results together establish that although dissociation is not affected by single-site mutation alone in this protein system, ligand binding exerts a greater influence on the unfolding of the variant compared to the wild-type protein.

Our measurements reveal that L55P has an unstable quaternary arrangement relative to WT TTR whereas the stability of tertiary and secondary structural elements is similar in both WT and L55P TTR, in the absence of ligands. This is in agreement with previous MS studies of amyloidogenic variants of TTR (Nettleton et al., 1998). The stability of tertiary structures in different variants of TTR has not been studied previously by MS, but unfolding of pathogenic variants of TTR by GdnHCl (guanidine hydrochloride) has indicated that a complicated denaturation pathway exists for L55P (Hurshman Babbes et al., 2008). In addition, we observe that ligand binding affords different stabilities to variant and WT TTR. It is established crystallographically that ligands bind to TTR in the central channel and hydrogen bond

with Lys15 and Glu54. This results in a more compact TTR-ligand complex compared to apo-TTR (Wojtczak et al., 1996) and is consistent with previous observations that L55P TTR upon ligand binding decreases in size to a greater extent than WT TTR (Morais-de-Sa et al., 2006). Although this subtle compaction was not observed in our experiments, our results provide direct evidence for the enhanced stability of the holo-TTR complex afforded by ligand binding. It is likely that the relative instability of the variant tetramer complex allows the unfolding reaction to proceed at lower energies compared with the WT complex. Consequently, the unfolding reaction for the variant TTR proceeds more slowly, allowing observation of partially unfolded intermediates not apparent in the WT unfolding (Baer and Mayer, 1997). Overall, therefore, our data highlight the ability of IM-MS to distinguish clearly the disruption of tertiary elements from the dissociation of the tetrameric assembly.

The differential influence of ligands on variant and WT TTR is illustrated schematically using data acquired for TTR-L$_2$ forms of WT and L55P TTR (Figure 6). The scheme describes the preference of the TTR tetramer to unfold or dissociate upon activation. Also shown are dissociative products from a given state of the unfolded tetramer. We cannot define explicitly the structures of these unfolded conformational ensembles, but we have limited unfolding pathways to that of a single monomer in the light of previous experimental results (Ruotolo et al., 2007). For WT TTR, the intact tetramer-ligand assembly begins to unfold as the assembly is activated. Significant unfolding of the tetramer precedes dissociation. In contrast, the dissociation of L55P TTR does not require significant unfolding of monomeric units prior to dissociation, and thus ejection of a monomer
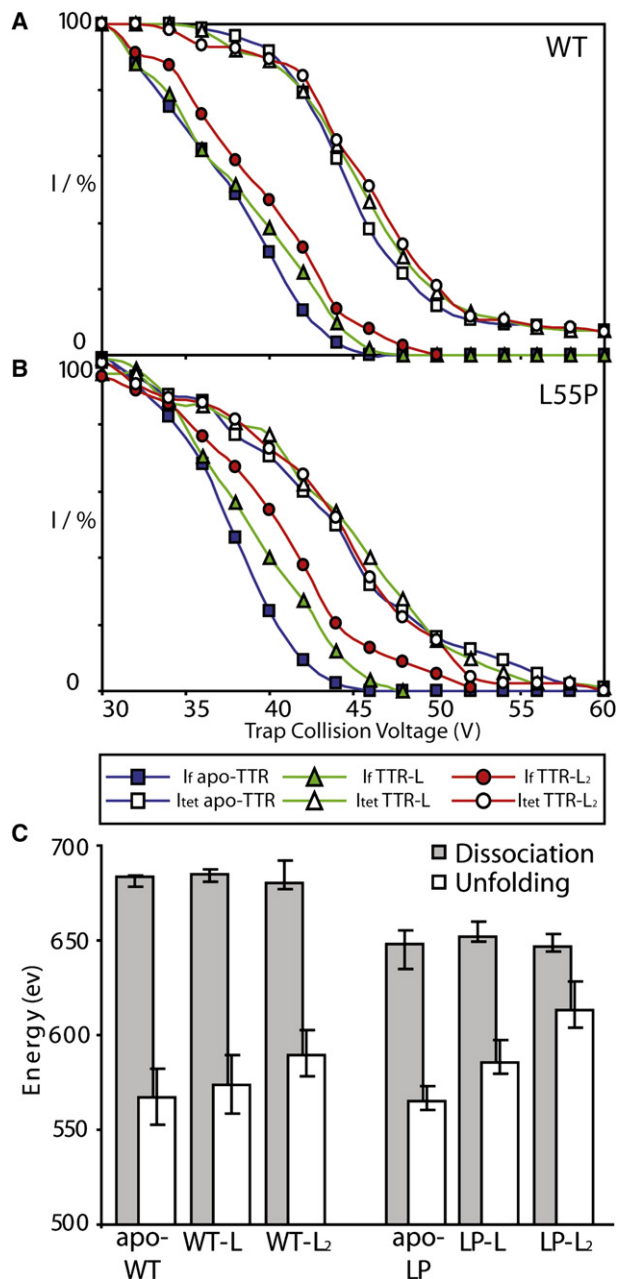
A

B

C

Figure 5. Elucidating the Extent of Unfolding and Dissociation from IM-MS

Plots of I_f and I_{tet} across a range of activation voltages for 15+ charge states of WT (A) and L55p (B) TTR. A plot of the 50% dissociation yield (gray) and unfolding yield (white) for wild-type and L55P TTR tetramers is reported within ± 1 SD (C). The average experimental error on the laboratory-frame energy axis is ~±5 eV.

Figure 6. Schematic Representation of Unfolding and Dissociation Pathway for WT and L55P TTR in Complex with Ligands

The vertical axis represents the extent of unfolding of an initially compact tetramer, and the horizontal axis represents the extent of dissociation (i.e., the inverse of % intact tetramer surviving after activation). Activation results in gradual unfolding of the tetramer. This leads to an expulsion of significantly unfolded subunits in the case of WT TTR tetramers, or to a greater range of partially unfolded monomers in the case of L55P TTR. Illustrative representations of the dissociation products generated from a given state of unfolded tetramer-ligand complex are located on the unfolding/dissociation trajectory shown for each tetramer (circles).

SIGNIFICANCE

In this report, we studied TTR and its disease-associated variants in complex with its natural ligand, thyroxine. Using IM-MS, we show that IM can provide a complementary data set to MS for ligand-binding experiments. By isolating and activating different ligated states, we have shown that TTR uniformly unfolds into at least five different structural ensembles that are stable on a millisecond timescale. The ability to detect these structural ensembles is seemingly unaffected by point mutation or ligand binding, allowing us to construct a robust IM-MS unfolding "fingerprint" for TTR. We propose that this fingerprint concept may be translated to other protein assemblies and used as a general approach to ascertain the relative stability afforded to a protein as a consequence of ligand binding.

Furthermore, our IM-MS data show that the unfolding of TTR can be decoupled from the dissociation of the tetramer. The more amyloidogenic variant of TTR, L55P, dissociates, having undergone less unfolding relative to WT TTR. We also demonstrate that individual ligand-binding stoichiometries of TTR can be isolated from a mixture of ligand-bound states and interrogated independently. Our results show that TTR is stabilized in an additive manner with successive ligand binding. In addition, the L55P variant TTR was more resistant to unfolding as a result of ligand binding than WT TTR. With the ability to interrogate an individual ligated state of a multiprotein complex, IM-MS provides an unprecedented opportunity for studying a heterogeneous system possessing multiple binding stoichiometries for ligands. Together with data from other complementary techniques

occurs at lower-accelerating voltages than the analogous reaction in the WT protein. We propose that this difference is due to the weaker protein-protein contacts in L55P compared to WT TTR, leading to greater dissociation, whereas the unfolding within individual subunits is similar to that shown previously (Ruotolo et al., 2007). Taken together, the data presented here demonstrate how IM-MS can provide an information set capable of describing the stability of multiprotein complexes in a detailed way.
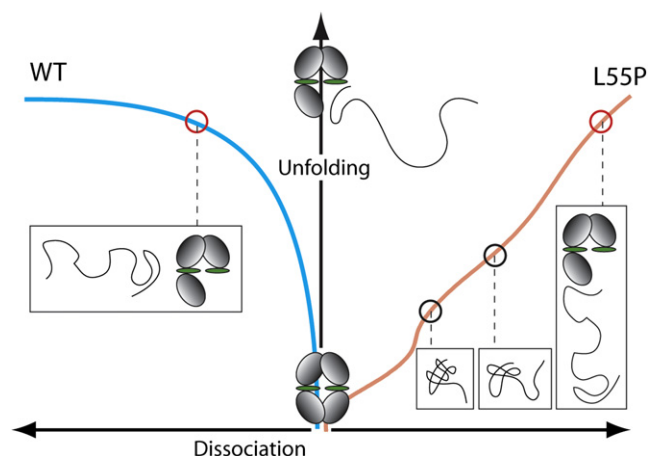
(Felitsyn et al., 2001; Shoemaker et al., 2007), we anticipate that this approach will be able to elucidate interactions within multiprotein-ligand complexes, as well as provide further evidence as to the applicability of gas-phase data to problems in structural biology (Ruotolo and Robinson, 2006).

EXPERIMENTAL PROCEDURES

Protein Expression and Reagents

Recombinant human wild-type and variant (L55P, V30M, and T119M) transthyretin were expressed and purified as previously described (Lashuel et al., 1998). Isotopically labeled transthyretin was expressed in minimal medium with [^{15}N]ammonium chloride and [^{13}C]glucose (Spectra Stable Isotopes) as the sole nitrogen and carbon sources, respectively. The identity of each preparation was confirmed by ESI-mass spectrometry. L-thyroxine, dimethyl sulfoxide (DMSO), and ammonium acetate were purchased from Sigma unless otherwise stated.

Sample Preparation for Mass Spectrometry

The proteins were buffer exchanged into 20 mM ammonium acetate (pH 7.0) using micro Bio-spin 6 columns (Bio-Rad). For all experiments the concentration of protein tetramer was 3.60 μM. In studying the effect of point mutation, two solutions were analyzed to eliminate bias due to labeling TTR with heavy isotopes: wild-type [^{12}C-^{14}N]transthyretin + L55P [^{13}C-^{15}N]transthyretin and L55P [^{12}C-^{14}N]transthyretin + wild-type [^{13}C-^{15}N] transthyretin. For the study of ligand binding, L-thyroxine was prepared as a stock solution in DMSO at a concentration of 1.60 mM. It was added to either wild-type or L55P transthyretin to a concentration of 3.24 μM. In addition, L-thyroxine was added to a solution of wild-type [^{12}C-^{14}N]transthyretin and wild-type [^{13}C-^{15}N]transthyretin to ascertain that ligands bind with the same affinity under mass spectrometry analysis.

Ion Mobility-Mass Spectrometry

Mass spectrometry and ion-mobility measurements were carried out on a Synapt HDMS (Waters, Manchester, UK) quadrupole-ion trap-IM-MS instrument. Nanoflow electrospray capillaries were prepared as previously described (Hernandez and Robinson, 2007). TTR ions were generated using a nanoflow electrospray (nano-ESI) source. To preserve the noncovalent interactions in the apo and holo forms of transthyretin, the MS parameters were adjusted to the following values: capillary voltage, 1.0 kV; sample cone, 80 V; cone gas, 130 l hr^{-1}; trap collision voltage, 25 V; ion-transfer stage pressure, 5.50 millibars; time-of-flight analyzer pressure, 2.15 × 10^{-6} millibars. Under these conditions, no dissociation of the tetramer was observed in the mass spectrum. For CID-induced activation, the trap collision voltage (the bias voltage that alters the amount of energy provided to the ions as they enter the ion trap prior to IM separation) was varied during the acquisition of spectra while keeping other settings constant.

In tandem-MS mode, ions of a narrow range of mass at either 3720, 3775, or 3825 m/z were selected in the first quadrupole mass analyzer prior to accumulation in the ion trap for ligand-binding experiments. The selected ions correspond to 15+ charge state of unbound TTR (apo-TTR) and TTR-ligand complex (apo-TTR) with one and two ligands, respectively. In the case of the experiment to compare wild-type and variant TTR, ions were selected in the quadrupole mass analyzer at an m/z of either 3720 or 3900, which corresponds to 15+ charge state of transthyretin without or with isotope labels.

Each of these mass-selected ions was interrogated by changing the trap collision voltage in the ion trap just prior to the mobility cell. The increased voltage accelerates the ions such that they encounter neutral gas molecules with greater kinetic energy in the ion trap. Low voltage waves propagate at a fixed frequency in the ion mobility region and separate the ions according to their collision cross-section (Pringle et al., 2007). A single drift tube separation takes 30 ms, during which 200 time-of-flight events can be recorded for the ions that exit the ion-mobility cell (maintained at a pressure of 0.5 mbar of N$_2$).

All mass spectra were calibrated externally using a solution of cesium iodide (100 mg ml^{-1}) and were processed with Masslynx 4.1 software (Waters, UK). Spectra are shown with minimal smoothing and without background subtrac-

tion. Drift time was converted into collision cross-sections using known values for partially unfolded structures for the 15+ charge state of the transthyretin tetramer and other proteins of known cross-sections (Ruotolo et al., 2007). The collision cross-sections of additional unfolded species, arising from the TTR-ligand complexes, were estimated from calibration with ions of known cross-sections (Ruotolo et al., 2008). The relative abundance of 15+ charge state of tetramer (I_{tet}) was calculated as a percentage of the total intensity of the peaks in the mass spectra assigned to 15+ charge state of tetrameric transthyretin and 6+ through 9+ charge state of monomeric transthyretin. In the case of TTR-L$_1$, which dissociates into monomers and trimers while losing its ligand and converting to the apo form (TTR), all tetrameric MS signal intensity was combined to estimate the extent of tetrameric ion signal. The relative abundance of the compact 15+ charge state of tetrameric transthyretin separated by ion-mobility cell (I_f) was calculated as a percentage of the total intensity of the peaks in the arrival time distribution:

$$I_{tet}(\%) = \frac{I_{tet}}{I_{tet} + I_{m\ on}} \times 100$$

$$I_f(\%) = \frac{I_{folded}}{\sum I_{conformers}} \times 100.$$

The magnitude of laboratory-frame energy applied to accelerate TTR tetramer ions was estimated by multiplying the trap collision voltage by the number of charges on the ion (Laskin and Futrell, 2005).

SUPPLEMENTAL DATA

Supplemental Data include three figures, one table, and Supplemental Experimental Procedures and can be found with this article online at http://www.cell.com/chemistry-biology/supplemental/S1074-5521(09)00074-X.

REFERENCES

Baer, T., and Mayer, P.M. (1997). Statistical Rice-Ramsperger-Kassel-Marcus quasiequilibrium theory calculations in mass spectrometry. J. Am. Soc. Mass Spectrom. 8, 103–115.

Benesch, J.L., Aquilina, J.A., Ruotolo, B.T., Sobott, F., and Robinson, C.V. (2006). Tandem mass spectrometry reveals the quaternary organization of macromolecular assemblies. Chem. Biol. 13, 597–605.

Blake, C.C., Geisow, M.J., Oatley, S.J., Rerat, B., and Rerat, C. (1978). Structure of prealbumin: secondary, tertiary and quaternary interactions determined by Fourier refinement at 1.8 Å. J. Mol. Biol. 121, 339–356.

Bovet, C., Wortmann, A., Eiler, S., Granger, F., Ruff, M., Gerrits, B., Moras, D., and Zenobi, R. (2007). Estrogen receptor-ligand complexes measured by chip-based nanoelectrospray mass spectrometry: an approach for the screening of endocrine disruptors. Protein Sci. 16, 938–946.

Felitsyn, N., Kitova, E.N., and Klassen, J.S. (2001). Thermal decomposition of a gaseous multiprotein complex studied by blackbody infrared radiative dissociation. Investigating the origin of the asymmetric dissociation behavior. Anal. Chem. 73, 4647–4661.

Felitsyn, N., Kitova, E.N., and Klassen, J.S. (2002). Thermal dissociation of the protein homodimer ecotin in the gas phase. J. Am. Soc. Mass Spectrom. 13, 1432–1442.

Ganem, B., Li, Y.T., and Henion, J.D. (1991). Observation of noncovalent enzyme-substrate and enzyme-product complexes by ion-spray mass spectrometry. J. Am. Chem. Soc. 113, 7818–7819.

Hammarstrom, P., Wiseman, R.L., Powers, E.T., and Kelly, J.W. (2003). Prevention of transthyretin amyloid disease by changing protein misfolding energetics. Science 299, 713–716.

Hernandez, H., and Robinson, C.V. (2007). Determining the stoichiometry and interactions of macromolecular assemblies from mass spectrometry. Nat. Protoc. 2, 715–726.

Hoaglund-Hyzer, C.S., Counterman, A.E., and Clemmer, D.E. (1999). Anhydrous protein ions. Chem. Rev. 99, 3037–3079.

Hu, P., and Loo, J.A. (1995). Determining calcium-binding stoichiometry and cooperativity of parvalbumin and calmodulin by mass spectrometry. J. Mass Spectrom. 30, 1076–1082.

Hurshman Babbes, A.R., Powers, E.T., and Kelly, J.W. (2008). Quantification of the thermodynamically linked quaternary and tertiary structural stabilities of transthyretin and its disease-associated variants: the relationship between stability and amyloidosis. Biochemistry 47, 6969–6984.

Jarrold, M.F. (2000). Peptides and proteins in the vapor phase. Annu. Rev. Phys. Chem. 51, 179–207.

Jurchen, J.C., and Williams, E.R. (2003). Origin of asymmetric charge partitioning in the dissociation of gas-phase protein homodimers. J. Am. Chem. Soc. 125, 2817–2826.

Jurchen, J.C., Garcia, D.E., and Williams, E.R. (2004). Further studies on the origins of asymmetric charge partitioning in protein homodimers. J. Am. Soc. Mass Spectrom. 15, 1408–1415.

Katta, V., and Chait, B.T. (1991). Observation of the heme-globin complex in native myoglobin by electrospray-ionization mass spectrometry. J. Am. Chem. Soc. 113, 8534–8535.

Keetch, C.A., Bromley, E.H., McCammon, M.G., Wang, N., Christodoulou, J., and Robinson, C.V. (2005). L55P transthyretin accelerates subunit exchange and leads to rapid formation of hybrid tetramers. J. Biol. Chem. 280, 41667–41674.

Kitova, E.N., Seo, M., Roy, P.N., and Klassen, J.S. (2008). Elucidating the intermolecular interactions within a desolvated protein-ligand complex. An experimental and computational study. J. Am. Chem. Soc. 130, 1214–1226.

Klabunde, T., Petrassi, H.M., Oza, V.B., Raman, P., Kelly, J.W., and Sacchettini, J.C. (2000). Rational design of potent human transthyretin amyloid disease inhibitors. Nat. Struct. Biol. 7, 312–321.

Lashuel, H.A., Lai, Z., and Kelly, J.W. (1998). Characterization of the transthyretin acid denaturation pathways by analytical ultracentrifugation: implications for wild-type, V30M, and L55P amyloid fibril formation. Biochemistry 37, 17851–17864.

Laskin, J., and Futrell, J.H. (2005). Activation of large ions in FT-ICR mass spectrometry. Mass Spectrom. Rev. 24, 135–167.

Light-Wahl, K.J., Schwartz, B.L., and Smith, R.D. (1994). Observation of the noncovalent quaternary associations of proteins by electrospray ionization mass spectrometry. J. Am. Chem. Soc. 116, 5271–5278.

Loo, J.A. (1997). Studying noncovalent protein complexes by electrospray ionization mass spectrometry. Mass Spectrom. Rev. 16, 1–23.

McCammon, M.G., Scott, D.J., Keetch, C.A., Greene, L.H., Purkey, H.E., Petrassi, H.M., Kelly, J.W., and Robinson, C.V. (2002). Screening transthyretin amyloid fibril inhibitors: characterization of novel multiprotein, multiligand complexes by mass spectrometry. Structure 10, 851–863.

Morais-de-Sa, E., Neto-Silva, R.M., Pereira, P.J., Saraiva, M.J., and Damas, A.M. (2006). The binding of 2,4-dinitrophenol to wild-type and amyloidogenic transthyretin. Acta Crystallogr. D Biol. Crystallogr. 62, 512–519.

Nettleton, E.J., Sunde, M., Lai, Z., Kelly, J.W., Dobson, C.M., and Robinson, C.V. (1998). Protein subunit interactions and structural integrity of amyloidogenic transthyretins: evidence from electrospray mass spectrometry. J. Mol. Biol. 281, 553–564.

Nilsson, S.F., Rask, L., and Peterson, P.A. (1975). Studies on thyroid hormone-binding proteins. II. Binding of thyroid hormones, retinol-binding protein, and fluorescent probes to prealbumin and effects of thyroxine on prealbumin subunit self-association. J. Biol. Chem. 250, 8554–8563.

Pringle, S.D., Giles, K., Wildgoose, J.L., Williams, J.P., Slade, S.E., Thalassinos, K., Bateman, R.H., Bowers, M.T., and Scrivens, J.H. (2007). An investigation of the mobility separation of some peptide and protein ions using a new hybrid quadrupole/travelling wave IMS/oa-ToF instrument. Int. J. Mass Spectrom. 261, 1–12.

Robinson, C.V., Chung, E.W., Kragelund, B.B., Knudsen, J., Aplin, R.T., Poulsen, F.M., and Dobson, C.M. (1996). Probing the nature of non-covalent interactions by mass spectrometry. A study of protein-CoA ligand binding and assembly. J. Am. Chem. Soc. 118, 8646–8653.

Ruotolo, B.T., and Robinson, C.V. (2006). Aspects of native proteins are retained in vacuum. Curr. Opin. Chem. Biol. 10, 402–408.

Ruotolo, B.T., Giles, K., Campuzano, I., Sandercock, A.M., Bateman, R.H., and Robinson, C.V. (2005). Evidence for macromolecular protein rings in the absence of bulk water. Science 310, 1658–1661.

Ruotolo, B.T., Hyung, S.J., Robinson, P.M., Giles, K., Bateman, R.H., and Robinson, C.V. (2007). Ion mobility-mass spectrometry reveals long-lived, unfolded intermediates in the dissociation of protein complexes. Angew. Chem. Int. Ed. Engl. 46, 8001–8004.

Ruotolo, B.T., Benesch, J.L., Sandercock, A.M., Hyung, S.J., and Robinson, C.V. (2008). Ion mobility-mass spectrometry analysis of large protein complexes. Nat. Protoc. 3, 1139–1152.

Sebastiao, P., Dauter, Z., Saraiva, M.J., and Damas, A.M. (1996). Crystallization and preliminary X-ray diffraction studies of Leu55Pro variant transthyretin. Acta Crystallogr. D Biol. Crystallogr. 52, 566–568.

Shoemaker, G.K., Kitova, E.N., Palcic, M.M., and Klassen, J.S. (2007). Equivalency of binding sites in protein-ligand complexes revealed by time-resolved tandem mass spectrometry. J. Am. Chem. Soc. 129, 8674–8675.

Sobott, F., and Robinson, C.V. (2004). Characterizing electrosprayed biomolecules using tandem-MS—the noncovalent GroEL chaperonin assembly. Int. J. Mass Spectrom. 256, 25–32.

von Helden, G., Wyttenbach, T., and Bowers, M.T. (1995). Conformation of macromolecules in the gas phase: use of matrix-assisted laser desorption methods in ion chromatography. Science 267, 1483–1485.

Wojtczak, A., Cody, V., Luft, J.R., and Pangborn, W. (1996). Structures of human transthyretin complexed with thyroxine at 2.0 Å resolution and 3′,5′-dinitro-N-acetyl-L-thyronine at 2.2 Å resolution. Acta Crystallogr. D Biol. Crystallogr. 52, 758–765.